Ueda Y, Mizutani C, Nannya Y, Kurokawa M, Kobayashi S, Takeuchi J, Tamura H, Ogata K, Dan K, Shibayama H, Kanakura Y, Niimi K, Sasaki K, Watanabe M, Emi N, Teramura M, Motoji T, Kida M, Usuki K, Takada S, Sakura T, Ito Y, Ohyashiki K, Ogawa H, Suzuki T, Ozawa K, Imai K, Kasai M, Hata T, Miyazaki Y, Morita Y, Kanamaru A, Matsuda A, Tohyama K, Koga D, Tamaki H, Mitani K, Naoe T, Sugiyama H, Takaku F	Clinical evaluation of WT1 mRNA expression levels in peripheral blood and bone marrow in patients with myelodysplastic syndromes	Leuk Lymphoma	54	1450-1458	2013
Matsuda A, Jinnai I, Iwanaga M, Okamura D, Ishikawa M, Maeda T, Hata T, Kawai N, Miyazaki Y, Bessho M, Tomonaga M	Correlation Between Dysplastic Lineage and Type of Cytopenia in Myelodysplastic Syndromes Patients With Refractory Anemia According to the FAB Classification	Am J Clin Pathol	140	253-257	2013
Iriyama N, Hatta Y, Takeuchi J, Ogawa Y, Ohtake S, Sakura T, Mitani K, Ishida F, Takahashi M, Maeda T, Izumi T, Sakamaki H, Miyawaki S, Honda S, Miyazaki Y, Taki T, Taniwaki M, Naoe T	CD56 expression is an independent prognostic factor for relapse in acute myeloid leukemia with t(8;21)	Leuk Res	37	1021-1026	2013
Yanada M, Ohtake S, Miyawaki S, Sakamaki H, Sakura T, Maeda T, Miyamura K, Asou N, Oh I, Miyatake J, Kanbayashi H, Takeuchi J, Takahashi M, Dobashi N, Kiyoi H, Miyazaki Y, Emi N, Kobayashi Y, Ohno R, Naoe T; for the Japan Adult Leukemia Study Group	The demarcation between younger and older acute myeloid leukemia patients: A pooled analysis of 3 prospective studies	Cancer	119	3326-3333	2013
Fujita H, Asou N, Iwanaga M, Hyo R, Nomura S, Kiyoi H, Okada M, Inaguma Y, Matsuda M, Yamauchi T, Ohtake S, Izumi T, Nakaseko C, Ishigatsubo Y, Shinagawa K, Takeshita A, Miyazaki Y, Ohnishi K, Miyawaki S, Naoe T; the Japan Adult Leukemia Study Group	Role of hematopoietic stem cell transplantation for relapsed acute promyelocytic leukemia: A retrospective analysis of JALSG-APL97	Cancer Sci	104	1339-1345	2013
Hata T, Tsushima H, Baba M, Imaizumi Y, Taguchi J, Imanishi D, Nagai K, Tomonaga M, Miyazaki Y	Long-term outcome of immuno-suppressive therapy for Japanese patients with lower-risk myelodysplastic syndromes	Int J Hematol	98	687-693	2013

自治医科大学　　永井正　業績リスト

発表者名	論文タイトル名	発表誌名	巻号	ページ	出版年
Sripayap P, Nagai T, Uesawa M, Kobayashi H, Tsukahara T, Ohmine K, Muroi K & Ozawa K	Mechanisms of resistance to azacitidine in human leukemia cell lines	Exp Hematol, doi: 10.1016/j.exphem.2013.12.004			2014
Sripayap P, Nagai T & Ozawa K	Combined azacitidine and romidepsin enhances cytotoxicity in azacitidine-sensitive but not in azacitidine-resistant multiple myeloma cell lines	Jichi Medical University Journal	35	in press	2013
Sripayap P, Nagai T, Hatano K, Kikuchi J, Furukawa Y & Ozawa K	Romidepsin overcomes cell adhesion-mediated drug resistance in multiple myeloma cells	Acta Haematol	132	1-4	2014
Tatara R, Nagai T, Suzuki M, Oh I, Fujiwara S, Norizuki M, Muroi K & Ozawa K	Sepsis and meningoencephalitis caused by Bacillus cereus in a patient with myelodysplastic syndrome	Internal Med	52	1987-1990	2013
Nagai T, Karakawa M, Komine M, Muroi K, Ohtsuki M & Ozawa K	Development of psoriasis in a patient with chronic myelogenous leukemia during nilotinib treatment	Eur J Haematol	91	270-272	2013
Kobayashi H, Nagai T, Uesawa M, Fujiwara S, Matsuyama T, Sato K, Omine K, Ozaki K, Suzuki T, Mori M, Muroi K, Baley G, Yamamoto H & Ozawa K	Clinical outcome of non-surgical treatment for primary small intestinal lymphoma diagnosed with double-balloon endoscopy	Leuk Lymphoma	54	731-736	2013

Transforming mutations of RAC guanosine triphosphatases in human cancers

Masahito Kawazu[a], Toshihide Ueno[b], Kenji Kontani[c], Yoshitaka Ogita[c], Mizuo Ando[a], Kazutaka Fukumura[a], Azusa Yamato[b], Manabu Soda[b], Kengo Takeuchi[d], Yoshio Miki[e], Hiroyuki Yamaguchi[a], Takahiko Yasuda[a,f], Tomoki Naoe[f], Yoshihiro Yamashita[b], Toshiaki Katada[c], Young Lim Choi[a], and Hiroyuki Mano[a,b,g,1]

[a]Department of Medical Genomics, Graduate School of Medicine, University of Tokyo, Tokyo 113-0033, Japan; [b]Division of Functional Genomics, Jichi Medical University, Tochigi 329-0498, Japan; [c]Department of Physiological Chemistry, Graduate School of Pharmaceutical Sciences, University of Tokyo, Tokyo 113-0033, Japan; [d]Pathology Project for Molecular Targets, The Cancer Institute, Japanese Foundation for Cancer Research, Tokyo 135-8550, Japan; [e]Department of Genetic Diagnosis, The Cancer Institute, Japanese Foundation for Cancer Research, Tokyo 135-8550, Japan; [f]Department of Hematology and Oncology, Nagoya University Graduate School of Medicine, Nagoya 466-8550, Japan; and [g]Core Research for Evolutional Science and Technology, Japan Science and Technology Agency, Saitama 332-0012, Japan

Edited by Shuh Narumiya, Kyoto University Faculty of Medicine, Kyoto, Japan, and accepted by the Editorial Board January 9, 2013 (received for review September 22, 2012)

Members of the RAS superfamily of small guanosine triphosphatases (GTPases) transition between GDP-bound, inactive and GTP-bound, active states and thereby function as binary switches in the regulation of various cellular activities. Whereas HRAS, NRAS, and KRAS frequently acquire transforming missense mutations in human cancer, little is known of the oncogenic roles of other small GTPases, including Ras-related C3 botulinum toxin substrate (RAC) proteins. We show that the human sarcoma cell line HT1080 harbors both NRAS(Q61K) and RAC1(N92I) mutant proteins. Whereas both of these mutants were able to transform fibroblasts, knockdown experiments indicated that RAC1(N92I) may be the essential growth driver for this cell line. Screening for RAC1, RAC2, or RAC3 mutations in cell lines and public databases identified several missense mutations for RAC1 and RAC2, with some of the mutant proteins, including RAC1(P29S), RAC1(C157Y), RAC2(P29L), and RAC2(P29Q), being found to be activated and transforming. P29S, N92I, and C157Y mutants of RAC1 were shown to exist preferentially in the GTP-bound state as a result of a rapid transition from the GDP-bound state, rather than as a result of a reduced intrinsic GTPase activity. Activating mutations of RAC GTPases were thus found in a wide variety of human cancers at a low frequency; however, given their marked transforming ability, the mutant proteins are potential targets for the development of new therapeutic agents.

oncogene | resequencing

The identification of transforming proteins and the development of agents that target them have markedly influenced the treatment and improved the prognosis of individuals with cancer. Chronic myeloid leukemia (CML), for example, has been shown to result from the growth-promoting activity of the fusion tyrosine kinase breakpoint cluster region-Abelson murine leukemia viral oncogene homolog 1 (BCR-ABL1), and treatment with a specific ABL1 inhibitor, imatinib mesylate, has increased the 5-y survival rate of individuals with CML to almost 90% (1). Similarly, the fusion of echinoderm microtubule associated protein like 4 gene (*EML4*) to anaplastic lymphoma receptor tyrosine kinase (*ALK*) is responsible for a subset of non–small-cell lung cancer cases (2), and therapy targeted to EML4-ALK kinase activity has greatly improved the progression-free survival of affected individuals compared with that achieved with conventional chemotherapies (3). Therapies that target essential growth drivers in human cancers are thus among the most effective treatments for these intractable disorders.

V-Ki-ras2 Kirsten rat sarcoma viral oncogene homolog (KRAS), v-Ha-ras Harvey rat sarcoma viral oncogene homolog (HRAS), and neuroblastoma RAS viral (v-ras) oncogene homolog (NRAS) are the founding members of the rat sarcoma (RAS) superfamily of small guanosine triphosphatases (GTPases) that is known to comprise >150 members in humans (4). Five subgroups of these small GTPases have been identified and designated as the RAS; ras homolog family member (RHO); RAB1A, member RAS oncogene family (RAB); RAN, member RAS oncogene family (RAN); and ADP-ribosylation factor (ARF) families. All small GTPases function as binary switches that transition between GDP-bound, inactive and GTP-bound, active forms and thereby contribute to intracellular signaling that underlies a wide array of cellular activities, including cell proliferation, differentiation, survival, motility, and transformation (5). Somatic point mutations that activate KRAS, HRAS, or NRAS have been identified in a variety of human tumors, with KRAS being the most frequently activated oncoprotein in humans. Somatic activating mutations of KRAS are thus present in >90% of pancreatic adenocarcinomas, for example (6). Surprisingly, however, mutational activation of small GTPases other than KRAS, HRAS, and NRAS has not been widely reported.

Ras-related C3 botulinum toxin substrate (RAC) 1, RAC2, and RAC3 belong to the RHO family of small GTPases (7). RAC proteins orchestrate actin polymerization, and their activation induces the formation of membrane ruffles and lamellipodia (8), which play essential roles in the maintenance of cell morphology and in cell migration. Accumulating evidence also indicates that RAC proteins function as key hubs of intracellular signaling that underlies cell transformation. RAC1, for example, serves as an essential downstream component of the signaling pathway by which oncogenic RAS induces cell transformation, and artificial introduction of an amino acid substitution (G12V) into RAC1 renders it oncogenic (9). Furthermore, suppression of RAC1 activity induces apoptosis in glioma cells (10), and loss of *RAC1* or *RAC2* results in a marked delay in the development of BCR-ABL1–driven myeloproliferative disorder (11). Despite such important roles of RAC proteins in cancer, somatic transforming mutations of these proteins have not been identified in cancer specimens.

We have now discovered a mutant form of RAC1 with the amino acid substitution N92I in a human sarcoma cell line, HT1080, and have found that this mutation renders RAC1 constitutively active and highly oncogenic. Even though HT1080 cells also harbor the NRAS(Q61K) oncoprotein, RAC1(N92I) is the essential growth driver in this cell line, given that RNA interference (RNAi)-

Author contributions: M.K. and H.M. designed research; M.K., T.U., K.K., Y.O., M.A., K.F., A.Y., M.S., K.T., Y.M., H.Y., T.Y., T.N., Y.Y., T.K., and Y.L.C. performed research; M.K., T.U., K.K., Y.O., K.T., T.N., T.K., Y.L.C., and H.M. analyzed data; and H.M. wrote the paper.

The authors declare no conflict of interest.

This article is a PNAS Direct Submission. S.N. is a guest editor invited by the Editorial Board.

[1]To whom correspondence should be addressed. E-mail: hmano@m.u-tokyo.ac.jp.

This article contains supporting information online at www.pnas.org/lookup/suppl/doi:10.1073/pnas.1216141110/-/DCSupplemental.

mediated knockdown of RAC1(N92I) markedly suppressed cell growth. Further screening for *RAC1*, *RAC2*, and *RAC3* mutations among cancer cell lines as well as public databases identified additional transforming mutations of RAC1 and RAC2. Our data thus reveal oncogenic amino acid substitutions for the RAC subfamily of small GTPases in human cancer.

Results

Discovery of the RAC1(N92I) Oncoprotein. To identify transforming genes in the fibrosarcoma cell line HT1080 (12), we isolated cDNAs for cancer-related genes (n = 906) from HT1080 cells and subjected them to deep sequencing with the Genome Analyzer IIx (GAIIx) system. Quality filtering of the 92,025,739 reads obtained yielded 45,325,377 unique reads that mapped to 843 (93.0%) of the 906 target genes. The mean read coverage for the 843 genes was 495× per nucleotide, and ≥70% of the captured regions for 568 genes were read at ≥10× coverage.

Screening for nonsynonymous mutations in the data set with the use of our computational pipeline (13) revealed a total of five missense mutations with a threshold of ≥30× coverage and a ≥30% mutation ratio (Table S1). One of these mutations, a heterozygous missense mutation of *NRAS* that results in a Gln-to-Lys substitution at amino acid position 61 (Q61K), was described previously in this cell line (14) and is the most frequent transforming mutation of *NRAS* (5). We also discovered a missense mutation in another small GTPase, RAC1 (Fig. S1 and Table S1). An A-to-T transversion at position 516 of human *RAC1* cDNA (GenBank accession no. NM_006908.4), resulting in an Asn-to-Ile substitution at position 92 of the encoded protein, was thus identified in 11,525 (47.5%) of the 24,238 total reads covering this position.

To examine the transforming potential of RAC1(N92I), we infected mouse 3T3 fibroblasts and MCF10A human mammary epithelial cells (15) with a retrovirus encoding wild-type or N92I mutant form of human RAC1 and then seeded the cells in soft agar for evaluation of anchorage-independent growth. Neither 3T3 nor MCF10A cells expressing wild-type RAC1 grew in soft agar (Fig. 1*A*), indicating the lack of transforming potential of RAC1. In contrast, the cells expressing RAC1(N92I) readily grew in soft agar (Fig. 1*A*), showing that this RAC1 mutant confers the property of anchorage-independent growth on both 3T3 and MCF10A cells. We also confirmed the transforming potential of an artificial mutant of RAC1, RAC1(G12V) (8),

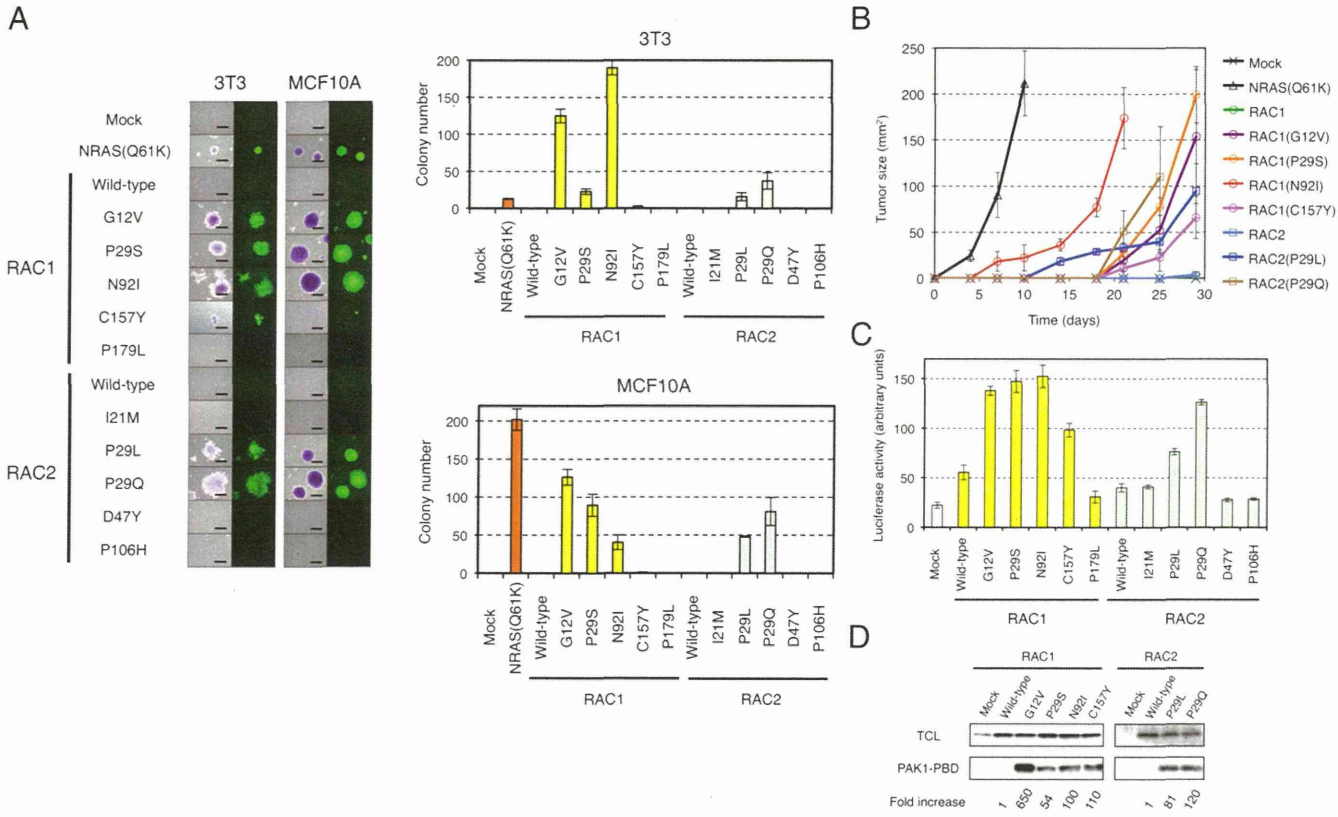

Fig. 1. Transforming potential of RAC1 and RAC2 mutants. (*A*) 3T3 or MCF10A cells were infected with recombinant retroviruses encoding enhanced green fluorescent protein (EGFP) as well as wild-type or mutant forms of RAC1 or RAC2 and were then assayed for anchorage-independent growth in vitro under the presence of 10% (vol/vol) FBS. After 14 d (3T3) or 20 d (MCF10A) of culture, the cells were stained with crystal violet and examined by conventional microscopy (*Left*: left image of each pair), and they were monitored for EGFP expression by fluorescence microscopy (*Left*: right image of each pair). (Scale bars, 0.5 mm.) The numbers of cell colonies were also determined as means ± SD from three independent experiments (*Right*). (*B*) 3T3 cells expressing wild-type or mutant forms of RAC1 or RAC2 were injected s.c. into the shoulder of nude mice, and the size of the resulting tumors [(length × width)/2] was determined at the indicated times thereafter. Tumor size for 3T3 expressing NRAS(Q61K) was similarly monitored. Data are means ± SD for tumors at four injection sites. (*C*) HEK293T cells were transfected with expression vectors for wild-type or mutant forms of RAC1 or RAC2 together with the SRE.L reporter plasmid and pGL-TK. The activity of firefly luciferase in cell lysates was then measured and normalized by that of *Renilla* luciferase. Data are means ± SD from three independent experiments. (*D*) Lysates of 3T3 cells expressing wild-type or mutant forms of RAC1 or RAC2 were subjected to a pull-down assay with PAK1-PBD. The precipitated proteins as well as the total cell lysates were then subjected to immunoblot analysis with antibodies to RAC1 or to RAC2. The relative amounts of pulled-down RAC proteins compared with their corresponding expression levels in total cell lysate were normalized to that of wild-type RAC1 (for the RAC1 mutants) or RAC2 (for the RAC2 mutants) and are shown at the bottom.

which harbors an amino acid substitution corresponding to that of the oncogenic G12V mutant form of RAS proteins.

Other Transforming Mutations of RAC1 and RAC2. We next searched for other transforming mutations of RAC proteins. Human RAC1, RAC2 (GenBank accession no. NM_002872.3), and RAC3 (GenBank accession no. NM_005052.2) cDNAs were isolated from 40 cancer cell lines (Table S2), and their nucleotide sequences were determined by Sanger sequencing, resulting in the discovery of RAC1(P29S), RAC2(P29Q), and RAC2(P29L) in the breast cancer cell line MDA-MB-157, the CML cell line KCL-22, and the breast cancer cell line HCC1143, respectively (Fig. S1 and Table S3). Further searching for *RAC1*, *RAC2*, and *RAC3* mutations in the COSMIC database of cancer genome mutations (Release V59; http://cancer.sanger.ac.uk/cancergenome/projects/cosmic) revealed various amino acid substitutions detected in human tumors, namely RAC1(P29S), RAC1(C157Y), RAC1(P179L), RAC2(I21M), RAC2(P29L), RAC2(D47Y), and RAC2(P106H) (Table S3). Importantly, all of these *RAC1* and *RAC2* mutations identified in clinical specimens were confirmed to be somatic, given that the corresponding mutations were absent in the genome of paired normal cells.

To examine the transforming potential of these various RAC1 and RAC2 mutants, we expressed each protein in 3T3 and MCF10A cells and evaluated anchorage-independent growth. Whereas the wild-type form of RAC2 did not transform 3T3 or MCF10A cells, growth in soft agar was apparent for 3T3 cells expressing RAC1 (P29S), RAC1(C157Y), RAC2(P29L), or RAC2(P29Q), but not for those expressing RAC1(P179L), RAC2(I21M), RAC2(D47Y), or RAC2(P106H) (Fig. 1*A*). Of interest, colony number in the assay varied substantially in a manner dependent on the type of amino acid substitution as well as on cell type. RAC1(C157Y), for example, yielded fewer colonies in soft agar compared with the other transforming mutants. Furthermore, RAC1(P29S), which was identified in a breast cancer cell line, generated a larger number of colonies with MCF10A cells than with 3T3 cells. Conversely, RAC1(N92I), which was identified in a fibrosarcoma cell line, yielded a larger number of colonies with 3T3 cells than with MCF10A cells. The oncogenic activity of RAC1(P29S), RAC1 (N92I), RAC1(C157Y), RAC2(P29L), and RAC2(P29Q) mutants was further confirmed with a tumorigenicity assay in nude mice (Fig. 1*B*), with the activity of RAC1(N92I) being the most pronounced with regard to the transformation of 3T3 cells in this assay.

The colony number in soft agar for 3T3 cells expressing NRAS (Q61K) was fewer than that for the cells expressing oncogenic RAC1 or RAC2 mutants (Fig. 1*A*), whereas expression of these small GTPases was readily confirmed in 3T3 (Fig. S2). Interestingly, s.c. tumors from the same 3T3 cells expressing NRAS(Q61K) grew more rapidly than tumors expressing the RAC1/RAC2 mutants (Fig. 1*B*), indicating that the measured intensity of the transforming potential of GTPases may vary in a dependent manner on assay systems.

To examine whether such oncogenic potential is linked directly to the activation of RAC1 or RAC2, we investigated the activity of the mutant proteins with the use of a luciferase reporter plasmid that selectively responds to intracellular signaling evoked by RHO family GTPases (16). In concordance with the data from the soft agar and tumorigenicity assays, only the transforming mutants of RAC1 and RAC2 yielded a substantial level of luciferase activity in transfected HEK293T cells (Fig. 1*C*).

Activated RAC1 or RAC2 would be expected to be loaded with GTP. We therefore examined the GTP-binding status of the RAC1 and RAC2 oncoproteins with the use of a pull-down assay based on the p21-binding domain (PBD) of PAK1. All of the transforming RAC1 and RAC2 mutants were found to exist preferentially in the GTP-bound state (Fig. 1*D*), indicative of their constitutive activation. Furthermore, these RAC1 and RAC2 mutants induced marked reorganization of the actin cytoskeleton in 3T3 cells, resulting in the accumulation of polymerized actin in ruffles at the plasma membrane (Fig. 2).

RAC1 and RAC2 as Therapeutic Targets. Given that NRAS(Q61K) is also known to transform 3T3 cells (17) (Fig. 1*A*), our data show that HT1080 cells harbor two independent oncogenic GTPases. We therefore examined whether RAC1(N92I) or NRAS(Q61K) is the principal growth driver in this sarcoma cell line. Among several small interfering RNAs (siRNAs) designed to attenuate the expression of RAC1 or NRAS, we selected two independent siRNAs that specifically target each mRNA (Fig. 3*A*). Whereas transfection of HT1080 cells with either NRAS siRNA resulted in a moderate inhibition of cell proliferation under the presence of 10% (vol/vol) FBS, that with either RAC1 siRNA almost blocked cell growth (Fig. 3*B*). Transfection with an NRAS siRNA in addition to either RAC1 siRNA did not result in an additional effect on cell proliferation (Fig. 3*B*). Similar data were observed in a culture with 1% (vol/vol) FBS (Fig. S3*A*) or under FBS-free conditions (Fig. S3*B*). To further examine the effects of silencing RAC1/NRAS, we quantitated cell cycle distribution of HT1080 transfected with siRNAs against either RAC1 or NRAS. As shown in Fig. S4*A*, DNA synthesis was equally suppressed by the knockdown of RAC1 or NRAS. Interestingly, however, CASP3/CASP7 activity (a surrogate marker for apoptosis) was markedly induced only by RAC1 depletion (Fig. S4*B*). Therefore, RAC proteins are likely to provide RAS-independent cell survival

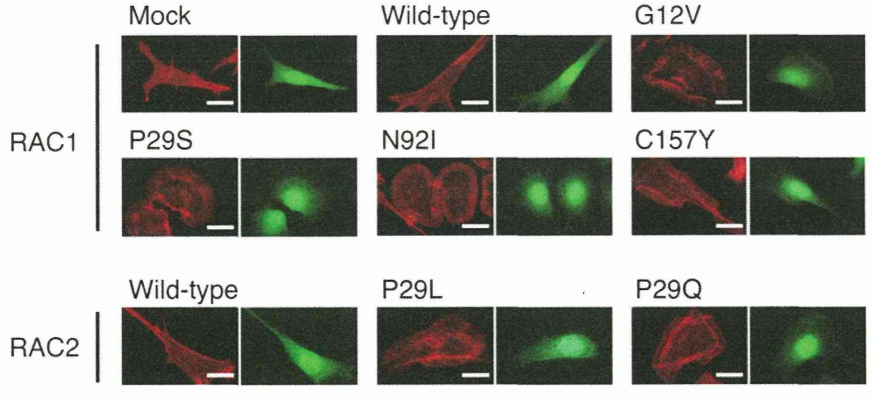

Fig. 2. Actin reorganization induced by the RAC1/RAC2 mutants. 3T3 cells infected with retroviruses encoding enhanced green fluorescent protein (EGFP) as well as wild-type or mutant forms of RAC1 or RAC2 were stained with Alexa Fluor 594-labeled phalloidin to visualize actin organization (*Left* image of each pair). The same cells were also examined for EGFP fluorescence (*Right* image of each pair). (Scale bars, 20 μm.)

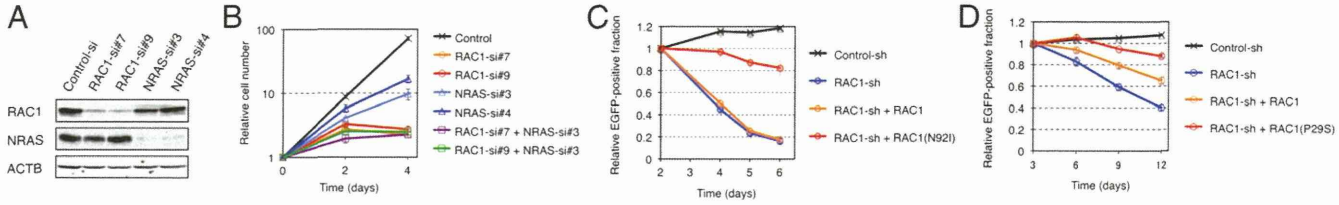

Fig. 3. Oncogenic RAC proteins as therapeutic targets. (*A*) HT1080 cells were transfected with control, RAC1, or NRAS siRNAs; lysed; and subjected to immunoblot analysis with antibodies to RAC1, NRAS, or ACTB (loading control). (*B*) HT1080 cells were transfected with control, RAC1, or NRAS siRNAs, as indicated, and cultured under the presence of 10% (vol/vol) FBS. Cell number was counted at the indicated times after the onset of transfection. Data are means ± SD from three independent experiments. (*C*) HT1080 cells were infected with a retrovirus encoding green fluorescent protein (EGFP) as well as a control or RAC1 shRNA. They were also infected with a retrovirus encoding shRNA-resistant wild-type RAC1 or RAC1(N92I), as indicated. The number of EGFP-positive cells was determined by flow cytometry after culture of the cells for the indicated times, and the size of the EGFP-positive fraction relative to that at 2 d was calculated. Data are means ± SD from three independent experiments. (*D*) MDA-MB-157 cells were infected with a retrovirus encoding EGFP as well as a control or RAC1 shRNA. They were also infected with a retrovirus encoding shRNA-resistant wild-type RAC1 or RAC1(P29S), as indicated. The number of EGFP-positive cells was determined by flow cytometry after culture of the cells for the indicated times, and the size of the EGFP-positive fraction relative to that at 3 d was calculated. Data are means ± SD from three independent experiments.

signals, which is supported by the fact that, even under FBS-free conditions, RAC1 depletion has more antiproliferative effects in HT1080 than NRAS depletion (Fig. S3*B*). These data show that active RAC1 may be the essential growth driver in HT1080 cells and is therefore a potential therapeutic target. Furthermore, our data suggest that oncogenic RAS proteins may require additional transforming hits to give rise to full-blown cancer.

We next infected HT1080 cells with a retrovirus expressing a short hairpin RNA (shRNA) targeted to RAC1 mRNA. Expression of the RAC1 shRNA markedly suppressed cell growth, whereas restoration of shRNA-resistant RAC1(N92I) expression reversed this effect (Fig. 3*C* and Fig. S5), showing that the effect of the RAC1 shRNA was not an off-target artifact. Forced expression of shRNA-resistant wild-type RAC1 failed to reverse the inhibitory effect of the RAC1 shRNA on cell growth, indicating that growth suppression by the shRNA was due to depletion of the N92I mutant, not to that of the wild-type protein. We performed similar experiments with the breast cancer cell line MDA-MB-157, which harbors RAC1(P29S). Again, the RAC1 shRNA inhibited cell growth, and this effect was reversed to a larger extent by restoration of the expression of shRNA-resistant RAC1(P29S) than by forced expression of the wild-type protein (Fig. 3*D* and Fig. S5).

RAC1(P29S), RAC1(N92I), and RAC1(C157Y) Are Rapid-Cycling Mutants. Oncogenic mutations at G12, G13, or Q61 of RAS proteins found in human tumors reduce the intrinsic GTPase activity of these

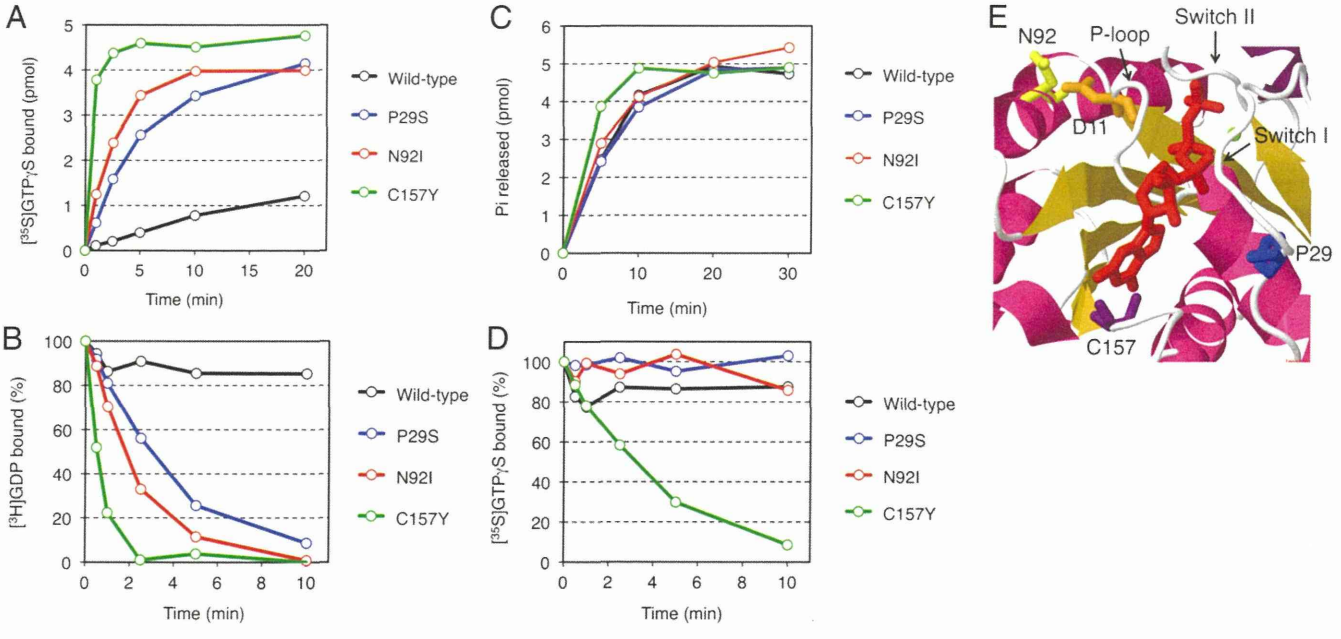

Fig. 4. Biochemical properties of RAC1 mutants. (*A*) Bacterially expressed and purified proteins of the wild-type, P29S, N92I, or C157Y mutant of RAC1 (5 pmol each) were incubated with [^{35}S]GTPγS in the presence of 0.8 mM Mg^{2+}, and the amounts of [^{35}S]GTPγS-bound proteins were determined at the indicated times. (*B*) [^{3}H]GDP dissociation from [^{3}H]GDP-bound RAC1 proteins was initiated by the addition of unlabeled GTPγS in the presence of 0.8 mM Mg^{2+}, and the amounts of [^{3}H]GDP-bound proteins were determined at the indicated times. (*C*) RAC1 proteins were preloaded with [γ^{32}P] GTP, and then GTP hydrolysis reactions were initiated by the addition of unlabeled GTP in the presence of 0.8 mM Mg^{2+}. P_i released from the proteins was isolated and measured at the indicated times. (*D*) [^{35}S]GTPγS dissociation from [^{35}S]GTPγS-bound RAC1 proteins was initiated by the addition of unlabeled GTPγS in the presence of 0.8 mM Mg^{2+}, and the amounts of [^{35}S]GTPγS-bound proteins were determined at the indicated times. (*E*) Schematic representation of the structure of the GTP-binding pocket of human RAC1 (ID 1mh1 in the Protein Data Bank; www.pdb.org) with α-helices and β-sheets shown in magenta and orange, respectively. The GTP analog guanosine 5′-(β,γ-imido)-triphosphate (GppNp) and Mg^{2+} are depicted in red and green, respectively. D11, P29, N92, and C157 amino acid residues are in orange, blue, yellow and purple, respectively. The positions of switch I and switch II regions and the P-loop are also indicated.

proteins and thereby maintain them in the GTP-bound state (18, 19). On the other hand, an artificial F28L substitution in HRAS or the RHO family protein Cdc42Hs was shown to confer constitutive activity by accelerating the transition from the GDP-bound to the GTP-bound state without the involvement of an exogenous guanine nucleotide exchange factor (GEF) (20, 21).

To determine how transforming mutations of RAC1 results in constitutive activation of these proteins, we examined their affinity for GTP and GDP. Compared with wild-type RAC1, all of RAC1(P29S), RAC1(N92I), and RAC1(C157Y) was found to bind GTPγS (nonhydrolyzable GTP analog) rapidly in vitro, even without the addition of a GEF protein (Fig. 4*A*). Likewise, the dissociation of GDP from the mutant forms of RAC1 was greatly accelerated (Fig. 4*B*). On the other hand, the intrinsic GTPase activity of these mutants was similar to (for P29S and N92I) or slightly higher (for C157Y) than that of the wild-type protein (Fig. 4*C*). These data thus indicated that, in contrast to transforming RAS mutants associated with human cancer, RAC1(P29S), RAC1(N92I), and RAC1(C157Y) are fast-cycling mutants, for which the probability of being in the GTP-bound state is increased as the result of an increased rate of GDP dissociation, rather than as the result of a loss of GTPase activity.

Interestingly, dissociation of GTPγS was also accelerated only for RAC1(C157Y), but not for the wild-type, P29S, or N92I form of RAC1 (Fig. 4*D*). Thus, RAC1(C157Y) is a unique mutant in that both association and dissociation for GTP are accelerated, which may provide the molecular basis for its modest transforming potential compared with that of RAC1(P29S) or RAC1(N92I) (Fig. 1).

In the 3D structure of RAC1 (Fig. 4*E*), P29 is located in the switch I region, whereas C157 is positioned adjacent to the guanine ring of bound GTP. Substitution of these residues would thus likely affect the affinity of the protein for GDP or GTP (Fig. S6), a phenomenon that has been demonstrated recently for RAC1 (P29S) (22). In contrast, N92 is located distant from the binding pocket for GDP/GTP, and so the structural mechanism by which the N92I substitution renders RAC1 constitutively active remains elusive (Fig. 4*E* and Fig. S6). Residue N92 is located close to D11 in the P-loop of RAC1, however (Fig. 4*E* and Fig. S7), and substitution with isoleucine at this position would abolish the interaction between the amino group of N92 and the carboxyl group of D11. It is thus possible that the N92I mutation affects the binding of GDP/GTP through an effect on the P-loop.

Discussion

We have here demonstrated the transforming potential of mutated RAC proteins. Our analysis of cell lines resulted in the identification of transforming mutants of RAC1 and RAC2, namely RAC1(N92I) and RAC2(P29Q), and we also revealed the transforming potential of the RAC1(P29S), RAC1(C157Y), and RAC2(P29L) mutants deposited the COSMIC database of cancer genome mutations (Release V59; http://cancer.sanger.ac.uk/cancergenome/projects/cosmic) (Table S3). In contrast, the soft agar assay did not reveal a transforming potential of the RAC1(P179L), RAC2(I21M), RAC2(D47Y), or RAC2(P106H) mutants found in the database, suggesting a possibility that they are "passenger mutations." It may also be possible, however, that these mutants may still contribute to cancer development by modifying tumor properties (such as metastasis ability), given that they were somatically acquired and clonally selected in cancer.

An important finding of our study was that the oncogenic effects of RAC1(N92I) may be more pronounced than those of NRAS(Q61K), at least with regard to survival signals in HT1080 cells (Fig. 3*B*). It should be noted, however, that HT1080 expresses RAC1 almost exclusively among the RAC family proteins, whereas HRAS and KRAS are weakly expressed in addition to NRAS (Fig. S8). It is thus possible that the effects of NRAS knockdown in Fig. 3*B* may be partly complemented by the residual HRAS/KRAS proteins.

Paterson et al. previously isolated NRAS-attenuated subclones of HT1080 after treatment with an alkylating reagent (*N*-methyl-*N*′-nitro-*N*-nitrosoguanidine) and a subsequent culture with 5-fluorodeoxyuridine and 1-β-D-arabinofuranosylcytosine (23). Such subclones had a flat cell shape and a reduced ability for anchorage-independent growth. Likewise, we noted that transfection with NRAS siRNAs renders HT1080 a flatter shape (Fig. S9). As demonstrated in Fig. 3*B* and by Paterson et al. (23), however, such NRAS-depleted HT1080 was still viable and kept proliferation in vitro, suggesting the presence of other oncogene(s) in addition to NRAS(Q61K). Therefore, NRAS(Q61K) and RAC1(N92I) are likely to cooperate to fully transform this fibrosarcoma.

Regarding the coexistence of mutations within RAC family proteins and RAS-RAF-MAPK proteins, two studies independently reported recurrent P29S mutation of RAC1 in melanoma during the preparation of this article (22, 24). Of note, BRAF (V600E) was also detected in four of six and in two of seven of the RAC mutation-positive melanomas, respectively. These observations, together with our findings with HT1080 cells, thus indicate that activating mutations of RAC1 and those of the RAS-RAF–signaling pathway are not mutually exclusive.

Members of the RAC subfamily of GTPases show a high level of sequence identity in humans. The amino acid sequence of RAC1 is thus 92% identical to that of RAC2 or RAC3. Furthermore, all of the amino acid residues of RAC1 or RAC2 found to be mutated in cancer (Table S3) are completely conserved among RAC1, RAC2, and RAC3. Thus, transforming RAC3 mutants with similar nonsynonymous mutations may also exist in human cancer, although such mutations were not detected in the current screening. Of interest, none of the frequent mutation sites in RAS family proteins (G12, G13, and Q61) were found to be affected in RAC1 or RAC2, although an artificial G12V mutant of RAC1 did manifest constitutive GTP loading and transforming potential. Given that RAC proteins perform intracellular functions (such as orchestration of the actin cytoskeleton) that are distinct from those of RAS family members, RAC-driven activation of specific intracellular pathways may be advantageous for cancer development in vivo.

Given that we detected activation mutations of RAC1 or RAC2 in cell lines from sarcoma (HT1080), triple-negative breast cancer (MDA-MB-157 and HCC1143), and the blast crisis stage of CML (KCL-22), we performed deep sequencing of *RAC1*, *RAC2*, and *RAC3* cDNAs with GAIIx for specimens of triple-negative breast cancer ($n = 66$), of *RAC1* and *RAC2* cDNAs for specimens of CML in blast crisis ($n = 43$), and of *BCR-ABL1*–positive acute lymphoblastic leukemia ($n = 31$), as well as of *RAC1* cDNAs for specimens of sarcoma ($n = 53$). We failed, however, to detect any nonsynonymous mutations among these RAC cDNAs.

Our results have shown that RAC proteins have the potential to become oncogenic through amino acid substitution in a wide array of cancers. Although such RAC mutations may occur at a low frequency, the recent studies of Krauthammer et al. (22) and Hodis et al. (24) suggest that they may be enriched in melanoma (~5%). Importantly, given that HT1080 cells are highly addicted to the increased activity of RAC1(N92I), the targeting of oncogenic RAC proteins or their downstream effectors with small compounds or RNAi may prove to be an effective approach to the treatment of cancer harboring such oncoproteins.

Materials and Methods

The human fibrosarcoma cell line HT1080 was obtained from American Type Culture Collection, and subjected to deep sequencing with GAIIx. Recombinant retrovirus expressing the wild-type or mutant forms of RAC1 or RAC2 was used to infect mouse 3T3 fibroblasts to examine its transforming potential. Detailed information for cDNA resequencing, transformation assays, biochemical analysis of RAC proteins, and RNAi are detailed in *SI Materials and Methods*.

ACKNOWLEDGMENTS. This study was supported in part by a grant for Research on Human Genome Tailor-Made from the Ministry of Health, Labor, and Welfare of Japan; Grants-in-Aid for Scientific Research (B) from the Japan Society for the Promotion of Science; and grants from The Yasuda Medical Foundation, The Sagawa Foundation for Promotion of Cancer Research, and The Mitsubishi Foundation.

1. Druker BJ, et al.; IRIS Investigators (2006) Five-year follow-up of patients receiving imatinib for chronic myeloid leukemia. *N Engl J Med* 355(23):2408–2417.
2. Soda M, et al. (2007) Identification of the transforming *EML4-ALK* fusion gene in non-small-cell lung cancer. *Nature* 448(7153):561–566.
3. Shaw AT, et al. (2011) Effect of crizotinib on overall survival in patients with advanced non-small-cell lung cancer harbouring ALK gene rearrangement: A retrospective analysis. *Lancet Oncol* 12(11):1004–1012.
4. Colicelli J (2004) Human RAS superfamily proteins and related GTPases. *Sci STKE* 2004 (250):RE13.
5. Cox AD, Der CJ (2010) Ras history: The saga continues. *Small GTPases* 1(1):2–27.
6. Jaffee EM, Hruban RH, Canto M, Kern SE (2002) Focus on pancreas cancer. *Cancer Cell* 2(1):25–28.
7. Wertheimer E, et al. (2012) Rac signaling in breast cancer: A tale of GEFs and GAPs. *Cell Signal* 24(2):353–362.
8. Ridley AJ, Paterson HF, Johnston CL, Diekmann D, Hall A (1992) The small GTP-binding protein rac regulates growth factor-induced membrane ruffling. *Cell* 70(3):401–410.
9. Qiu RG, Chen J, Kirn D, McCormick F, Symons M (1995) An essential role for Rac in Ras transformation. *Nature* 374(6521):457–459.
10. Senger DL, et al. (2002) Suppression of Rac activity induces apoptosis of human glioma cells but not normal human astrocytes. *Cancer Res* 62(7):2131–2140.
11. Thomas EK, et al. (2007) Rac guanosine triphosphatases represent integrating molecular therapeutic targets for BCR-ABL-induced myeloproliferative disease. *Cancer Cell* 12(5):467–478.
12. Rasheed S, Nelson-Rees WA, Toth EM, Arnstein P, Gardner MB (1974) Characterization of a newly derived human sarcoma cell line (HT-1080). *Cancer* 33(4):1027–1033.
13. Ueno T, et al. (2012) High-throughput resequencing of target-captured cDNA in cancer cells. *Cancer Sci* 103(1):131–135.
14. Hall A, Marshall CJ, Spurr NK, Weiss RA (1983) Identification of transforming gene in two human sarcoma cell lines as a new member of the ras gene family located on chromosome 1. *Nature* 303(5916):396–400.
15. Debnath J, Muthuswamy SK, Brugge JS (2003) Morphogenesis and oncogenesis of MCF-10A mammary epithelial acini grown in three-dimensional basement membrane cultures. *Methods* 30(3):256–268.
16. Hill CS, Wynne J, Treisman R (1995) The Rho family GTPases RhoA, Rac1, and CDC42Hs regulate transcriptional activation by SRF. *Cell* 81(7):1159–1170.
17. Marshall CJ, Hall A, Weiss RA (1982) A transforming gene present in human sarcoma cell lines. *Nature* 299(5879):171–173.
18. Adari H, Lowy DR, Willumsen BM, Der CJ, McCormick F (1988) Guanosine triphosphatase activating protein (GAP) interacts with the p21 ras effector binding domain. *Science* 240(4851):518–521.
19. Calés C, Hancock JF, Marshall CJ, Hall A (1988) The cytoplasmic protein GAP is implicated as the target for regulation by the ras gene product. *Nature* 332(6164): 548–551.
20. Reinstein J, Schlichting I, Frech M, Goody RS, Wittinghofer A (1991) p21 with a phenylalanine 28——leucine mutation reacts normally with the GTPase activating protein GAP but nevertheless has transforming properties. *J Biol Chem* 266(26): 17700–17706.
21. Lin R, Bagrodia S, Cerione R, Manor D (1997) A novel Cdc42Hs mutant induces cellular transformation. *Curr Biol* 7(10):794–797.
22. Krauthammer M, et al. (2012) Exome sequencing identifies recurrent somatic RAC1 mutations in melanoma. *Nat Genet* 44(9):1006–1014.
23. Paterson H, et al. (1987) Activated N-ras controls the transformed phenotype of HT1080 human fibrosarcoma cells. *Cell* 51(5):803–812.
24. Hodis E, et al. (2012) A landscape of driver mutations in melanoma. *Cell* 150(2): 251–263.

Leukemic evolution of donor-derived cells harboring *IDH2* and *DNMT3A* mutations after allogeneic stem cell transplantation

Leukemia (2014) **28,** 426–428; doi:10.1038/leu.2013.278

Although allogeneic stem cell transplantation is effective for the treatment of leukemia with poor prognosis, some such treated individuals experience disease relapse at various times after transplantation. Chimerism analysis of the relapsed disease has revealed infrequent cases in which the malignant cells originate from the donor and not from the initial leukemic clones.[1,2] Such donor cell leukemia (DCL) is often refractory to further treatment, with a mean overall survival for the affected patients of only 32.8 months.[2]

We recently described a 47-year-old Japanese man with acute myeloid leukemia (AML) who underwent a transplantation of peripheral blood stem cells (PBSCs) from his HLA-matched brother.[3] Although the allogeneic transplantation was successful, AML again became apparent in the patient 27 months later and chimerism analysis revealed that the leukemia was DCL. Genomic DNA was isolated and subjected to whole-exome sequencing from specimens of the initial AML (containing 70% myeloblasts, referred to as sample P1), the first complete remission after chemotherapy (sample P2), the first relapse (containing 24% myeloblasts; sample P3), donor PBSCs (sample D1), DCL at 27 months after allogeneic transplantation (containing 6% myeloblasts, sample D2) and DCL at 36 months after transplantation (containing 71% myeloblasts, sample D3).

Exome sequencing yielded a total of ~84.7 million, ~31.6 million, ~73.5 million, ~44.3 million and ~53.2 million unique, high-quality, paired-end reads for samples P1, P2, P3, D1 and D3, respectively (Supplementary Information). Although chimerism analysis for short tandem repeats had indicated that D3 was derived from D1 clones,[3] we further examined this possibility in a genome-wide manner. As demonstrated in Supplementary Figure 1a, the allele frequency of single-nucleotide polymorphisms (SNPs) detected in our data sets was highly concordant between P1 and P2 (Pearson's correlation coefficient (r) of 0.978) as well as between P1 and P3 ($r = 0.986$), suggesting that these three samples originate from a single individual. However, as expected, the concordance dropped substantially for the P1 and D3 pair ($r = 0.628$). In contrast, the concordance between D1 and D3 was high ($r = 0.983$), suggesting that the relapsed leukemia after transplantation was indeed derived from the donor cell. Of note, the allele frequency of SNPs showed only a low level of concordance ($r = 0.285$) between P1 and a cell line (KCL22)[4] derived from an unrelated Japanese patient with chronic myeloid leukemia (Supplementary Figure 1b). The correlation coefficient of 0.628 for P1 and D3 thus indicated that the patient and donor siblings share a substantial number of SNPs.

We next searched for somatic nonsynonymous mutations among the leukemic samples. For P1 and P3, we used P2 as a paired normal control. Given that D3 was shown to be derived from D1, we used the latter as the germline control for the former. Through our computational pipeline (Supplementary Information), nine missense mutations and two out-of-frame insertions/deletions (indels) were detected for P1, two missense mutations for P3 and nine missense mutations and one out-of-frame indel for D3 (Table 1). As described previously,[3] a 4-bp deletion of *CEBPA* was present in the initial AML but absent from the DCL. Similarly,

Table 1. Confirmed somatic mutations in the specimens analyzed

Specimen	*Gene symbol*	*GenBank accession no.*	*Nucleotide change*	*Amino-acid change*	*Mutation ratio (%)*				
					P1	*P2*	*P3*	*D1*	*D3*
P1	*ACSL5*	NM_016234	c.280G>A	p.V94I	40.6	0.0	30.6	0.0	0.0
	ANO4	NM_178826	c.2441C>T	p.S814L	42.3	0.0	16.7	0.0	0.0
	APOB	NM_000384	c.9175C>T	p.R3059C	32.8	0.0	7.4	0.0	0.0
	BANK1	NM_017935	c.222C>G	p.N74K	36.4	0.0	9.2	0.0	0.0
	CCDC88C	NM_001080414	c.3748G>A	p.E1250K	36.4	0.0	0.0	0.0	0.0
	FAM178B	NM_001122646	c.81G>A	p.M27I	41.2	0.0	25.0	0.0	0.0
	GABRB2	NM_021911	c.1009C>T	p.R337C	44.8	0.0	14.5	0.0	0.0
	JAK3	NM_000215	c.2570T>C	p.L857P	40.8	0.0	0.0	0.0	0.0
	SPATA31D1	NM_001001670	c.3793C>T	p.R1265C	36.6	0.0	6.7	0.0	0.0
	CEBPA	NM_004364	c.319_322delGACT	p.D107Tfs	63.6	0.0	10.0	0.0	0.0
	STAG2	NM_001042750	c.219_220insCG	p.H73Rfs	100.0	0.0	27.6	0.0	0.0
P3	*ACSL5*	NM_016234	c.280G>A	p.V94I	40.6	0.0	30.6	0.0	0.0
	NTNG2	NM_032536	c.1348G>T	p.G450C	0.0	0.0	37.5	0.0	0.0
D3	*CCDC168*	NM_001146197	c.11761G>C	p.D3921H	0.0	0.0	0.0	0.0	55.6
	GAL3ST1	NM_004861	c.1086G>T	p.M362I	0.0	0.0	0.0	0.0	32.6
	IDH2	NM_002168	c.419G>A	p.R140Q	0.0	0.0	0.0	7.1	50.0
	MYO7B	NM_001080527	c.635G>A	p.R212H	0.0	0.0	0.0	0.0	45.8
	NFATC1	NM_172390	c.736G>A	p.V246I	0.0	0.0	0.0	0.0	48.6
	PSMB8	NM_004159	c.637C>T	p.P213S	0.0	0.0	0.0	0.0	40.9
	TCAIM	NM_173826	c.668C>G	p.S223C	0.0	0.0	0.0	0.0	70.0
	TMEM132D	NM_133448	c.481G>A	p.A161T	0.0	0.0	0.0	0.0	35.3
	UBA2	NM_005499	c.419G>A	p.G140E	0.0	0.0	0.0	0.0	47.4
	DNMT3A	NM_153759	c.449delT	p.V150Gfs	0.0	0.0	0.0	8.7	61.1
	NRAS[a]	NM_002524	c.38G>A	p.G13D	0.0	0.0	0.0	0.0	18.4

[a]Below the threshold in the initial screening.

Accepted article preview online 26 September 2013; advance online publication, 15 October 2013

none of the identified somatic mutations were shared between the initial AML and DCL, providing further support for the distinct nature of the two leukemias.

Given that P3 contains only 24% myeloblasts, our computational pipeline could not accurately detect all of the associated somatic mutations. Indeed, most of the somatic mutations found in P1 (such as those in *ANO4*, *APOB*, *BANK1*, *STAG2* and *CEBPA*) were still present in P3 at lower frequencies (Table 1) but were not isolated in our pipeline analysis for P3. Lowering the threshold for somatic calls, however, increased the number of pseudopositive mutations in all specimens. We therefore applied the 30% threshold for mutation calls to all analyses. Of note, our data still indicate that P3 is not completely identical to P1. Nonsynonymous mutations of *CCDC88C* and *JAK3* detected in P1 were thus absent in P3, whereas a mutation of *NTNG2* was newly apparent in P3, suggestive of a clonal evolution in P3 divergent from the original P1 clones.

Surprisingly, whereas most somatic mutations detected in D3 were not present in D1, our results suggested that IDH2(R140Q) and DNMT3A(V150Gfs) were already present in the healthy donor at a low frequency (Table 1). Polymerase chain reaction (PCR)-based cloning of the genomic fragments and Sanger sequencing for *IDH2* and *DNMT3A* from D1 indeed confirmed the presence of the corresponding mutations in 2 (2.3%) out of 87 DNA clones and 1 (1.1%) out of 93 clones, respectively (Supplementary Figure 2). Furthermore, although the mutation rate (18.4%) was below the threshold of the present study, the oncogenic mutation NRAS(G13D)[5] in D3 (Table 1) was confirmed by Sanger sequencing of the corresponding genomic DNA (Supplementary Figure 2).

We then verified these infrequent mutations by sequencing the corresponding DNA fragments at extra-high coverage (hundreds of thousand times) with the use of a next-generation sequencer. The D2 sample, which contains only 6% myeloblasts, was also examined in this analysis. We confirmed that 1.6% (5.96×10^3 mutant reads out of 3.67×10^5 total reads at the corresponding nucleotide position) and 2.1% (1.24×10^4 out of 6.01×10^5 reads) of D1 cells already harbored the IDH2(R140Q) and DNMT3A(V150Gfs) mutations, respectively (Figure 1a). These mutations were not detected in the primary AML (P1 to P3). Whereas the *NRAS* mutation was not detected in D1, it became apparent in D2 and D3 at a frequency similar to that of the *IDH2* mutation. In addition, the *JAK3* mutation present in P1 was no longer evident at the relapsed stage P3.

On the basis of the genetic mutation profiles identified in the present case, we propose the following scheme for disease progression (Figure 1b). Given the high frequency of *STAG2* and *CEBPA* mutations in the primary AML, the 2-bp insertion in *STAG2* on the X chromosome (with there being only one copy of *STAG2* per cell in the male patient) as well as the heterozygous 4-bp deletion in *CEBPA* may characterize the founding clone of the original leukemia, with subsets of this clone subsequently acquiring additional oncogenic hits such as JAK3(L857P). The disappearance of *JAK3* and *CCDC88C* mutations in P3 suggests that the leukemic subclones harboring these mutations were sensitive to the initial chemotherapy.

The molecular pathogenesis of DCL has been unclear and may differ among cases. For instance, germline predisposition to cancer, such as the Li-Fraumeni syndrome or Bloom syndrome, may be shared between recipients and related donors.[6] However, in the present case, mutations in *IDH2* and *DNMT3A* were detected only in the donor, not in the primary AML, rendering this scenario unlikely. Alternatively, occult leukemia may already be present in the donor blood system and is inadvertently transmitted to the recipient.[7] In such cases, however, leukemia usually emerges in the donor soon after transplantation. Our donor, in contrast, has not developed any hematologic malignancy at 10 years after the donation of his PBSCs.

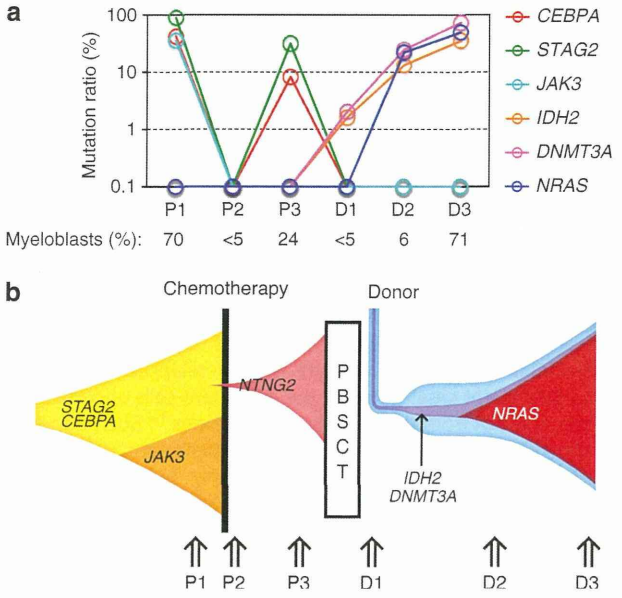

Figure 1. Genomic analysis of AML samples and donor PBSCs. (**a**) Genomic mutations corresponding to CEBPA(D107Tfs), STAG2(H73Rfs), JAK3(L857P), IDH2(R140Q), DNMT3A(V150Gfs) and NRAS(G13D) were examined by targeted deep sequencing in genomic DNA prepared from samples P1, P2, P3, D1, D2 and D3. The ratio of mutant reads to all reads at the corresponding position is shown as a percentage, with mutation frequencies of $<0.1\%$ being considered as 0.1% in the graph. The percentage of myeloblasts in each sample is indicated below the graph. (**b**) Founding clones of the primary AML harbored nonsynonymous mutations of *STAG2* and *CEBPA* and gave rise to subclones harboring a *JAK3* mutation. Whereas the latter cell population was sensitive to the initial chemotherapy, a subclone positive for an *NTNG2* mutation emerged from the former population and gave rise to relapse. All of these leukemic clones were successfully eradicated by peripheral blood stem cell transplantation (PBSCT). PBSCs of the donor, however, contained a small clonal population of cells positive for *IDH2* and *DNMT3A* mutations that eventually gave rise to AML on acquisition of additional mutations including NRAS(G13D).

Our present data therefore strongly suggest that apparently healthy individuals may harbor preleukemic subclones in their blood system (Figure 1b). Indeed, somatic mutations of *TET2* and *DNMT3A* were recently identified in clonal blood cells from one healthy elderly individual.[8] Furthermore, the *IDH2* and *DNMT3A* mutations identified in the present study may have had a specific role in the initiation of leukemia, given that mutations in the epigenetic modifiers including TET1/2, IDH1/2 and DNMT3A have been identified as early genetic events in AML progression.[9,10] Such mutations are indeed among the most frequently detected somatic alterations in AML.[11] These observations raise an important concern as to how 'appropriate' donors should be chosen, especially given that the incidence of DCL is increasing with the prevalence of molecular analysis for donor/recipient chimerism.[2] Prospective studies of whether and how examination of preleukemic subclones should be incorporated into the donor selection process for stem cell transplantation are thus warranted.

Furthermore, in our case, the oncogenic mutation NRAS(G13D) was likely a driver for leukemia progression, given that the frequency of this mutation was almost identical to that of the *IDH2* mutation in the D2 and D3 specimens. In contrast to the absence of leukemia in the donor, DCL rapidly developed in the recipient after transplantation in association with the accumulation of additional genetic hits, possibly as a result of a growth-promoting condition of the bone marrow after transplantation and due to a